Discover Oncology

Analysis

Role of the "inflammation-immunity-metabolism" network in non-small cell lung cancer: a multi-omics analysis

Jingqi Zhang[1,2] · **Liping Lin**[2] · **Wenyuan Li**[2] · **Jing Guo**[1]

Received: 2 March 2025 / Accepted: 12 May 2025
Published online: 21 May 2025

Abstract
Lung cancer remains one of the leading causes of cancer-related mortality, with non-small cell lung cancer (NSCLC) accounting for 85% of cases worldwide. NSCLC pathogenesis and progression are intricately linked to inflammatory stimuli, immune evasion, and metabolic reprogramming. In this study, the impact of inflammation, immunity, and metabolism on NSCLC was investigated by a Mendelian randomization analysis taking 91 inflammatory factors, 731 immune cells, and 1400 metabolites as exposures, and the FinnGen database NSCLC cohort (ncases = 5315, ncontrol = 314,193) was the outcome. A number of metabolites, inflammatory proteins, and immune cells were identified as potentially associated with NSCLC based on mendelian randomization analysis. Validation in the UK Biobank database lung cancer cohort (ncases = 2671, ncontrols = 372,016) further confirmed the inhibitory role of the metabolite N-acetyl-aspartyl-glutamate (NAAG) on lung cancer. Subsequently, single-cell and protein–protein interaction analyses identified inflammatory protein expression patterns in NSCLC, distribution ratios of immune cells in NSCLC. Subsequent multi-omics network analysis showed key interaction nodes between NAAG and inflammatory proteins. These findings enhance the understanding of the roles of inflammation, immunity, and metabolism in NSCLC occurrence and progression, offering potential targets and strategies for further research on its treatment and management.

Keywords Non-small cell lung cancer · Inflammation · Immunity · Metabolism · Multi-omics

Abbreviations

NSCLC	Non-small cell lung cancer
IL-6	Interleukin-6
IL-12B	IL-12 subunit beta
TNF-α	Tumor necrosis factor-alpha
Tregs	Regulatory T cells
CTLs	Cytotoxic T lymphocytes
NK	Natural killer
MR	Mendelian randomization
PPI	Protein–protein interaction
NAAG	*N*-Acetyl-aspartyl-glutamate

Supplementary Information The online version contains supplementary material available at https://doi.org/10.1007/s12672-025-02692-z.

✉ Jing Guo, guojing19910307@sina.com | [1]Hospital of Chengdu University of Traditional Chinese Medicine, Chengdu, China. [2]Chengdu University of Traditional Chinese Medicine, Chengdu, China.

SNPs	Single nucleotide polymorphisms
MAF	Minor allele frequency
IVs	Instrumental variables
IVW	Inverse variance weighted
FDR	False discovery rate
PLA	Phenyllactate
CCL11	Eotaxin
TSLP	Thymic stromal lymphopoietin
ADA	Adenosine deaminase
CD20 on IgD + CD38br	CD20 on IgD + CD38 + B cell
EM CD4 + AC	Effector memory CD4 + T cell absolute count
B cell AC	B cell absolute count
TD CD4 + %CD4 +	Terminally differentiated CD4 + T cell %CD4 + T cell
CCR2 on myeloid DC	CCR2 on myeloid dendritic cell
STAT1	Signal transducer and activator of transcription 1
UBC	Ubiquitin-conjugating enzyme E2 C
FoxO	Forkhead box O
MMP-2	Matrix metalloproteinase-2
ERK1/2	Extracellular signal-regulated kinases 1 and 2
JNK	C-Jun N-terminal kinases
ROS	Reactive oxygen species
PI3K/AKT	Phosphoinositide 3-kinase/protein kinase B
EMT	Epithelial-mesenchymal transition

1 Introduction

Lung cancer is a leading cause of cancer-related deaths, with non-small cell lung cancer (NSCLC) accounting for nearly 85% of all lung cancer cases globally [1]. In 2020, around 1.496 million deaths were estimated to be due to NSCLC, posing a significant threat to public health and imposing a substantial economic burden on the society [2].

The inflammatory stimuli, immune evasion, and metabolic reprogramming attributes in NSCLC progression are well-established. The tumor microenvironment (TME) of NSCLC was characterized by a persistent inflammatory state, with cytokines secreted by inflammatory cells, such as interleukin-6 (IL-6), IL-8, and tumor necrosis factor-*α* (TNF-*α*), which can influence the proliferative, angiogenic, and metastatic behaviors of tumor cells [3, 4]. On the other hand, elevated levels of C-reactive protein in patients with NSCLC are associated with poor prognosis [5]. Anti-inflammatory therapies as adjuncts to the comprehensive management of NSCLC hold promise. The TME in NSCLC often exhibits an expansion of immunosuppressive cells, such as regulatory T cells (Tregs) and M2 macrophages. This expansion is correlated with a concomitant suppression of both the quantity and activity of antitumor effector cells, including CD8 + cytotoxic T lymphocytes (CTLs) and natural killer (NK) cells. As a result, tumor cells are able to evade immune surveillance [6–8]. Tumor cell proliferation frequently accompanies metabolic reprogramming, including altered glucose [9] and lipid [10] metabolism, with over 150 metabolites found to be associated with metabolic changes in lung cancer [11]. Inflammation, immunity, and metabolism are intertwined in lung cancer, as enhanced inflammation (high proportions of cytotoxic and exhausted CD8 + T cells) can synergistically suppress immunity, leading to low muscle mass in patients with lung cancer [12]. Tumor-driven metabolic reprogramming can also induce changes in inflammation-associated proteins and immune cell levels, forming an "inflammation-immunity-metabolism" network.

Pathogenesis of NSCLC is complex, involving multiple aspects involving inflammation [13], immunity [14], and metabolism [15]. Most current studies focus on a specific biological dimension, such as employing circulating tumor DNA in plasma to identify putative mutational targets for guiding targeted therapy [16], evaluating the role of immunohistochemical markers in NSCLC [17], exploring the association between long non-coding RNAs and NSCLC treatment response [18], and investigating the relationship between different modes of cell death and lung cancer prognosis [19, 20]. Nevertheless, focusing on a single dimension may overlook potentially crucial pathogenic mechanisms and lead to suboptimal therapeutic outcomes. To overcome this limitation, a multi-omics integrative analysis strategy was employed in this study for an in-depth investigation of the molecular mechanisms underlying NSCLC.

To enhance the persuasiveness of the evidence, we utilized the large FinnGen dataset as the outcome and performed Mendelian randomization (MR) analyses in the inflammation, immune, and metabolic domains. We finally identified four inflammatory proteins, five immune cell types, and seven metabolites. Subsequently, we combined protein–protein interaction (PPI), and single-cell analyses to explore the roles of four identified inflammatory proteins and key immune cells (Effector Memory CD4 + T cells, B cells, etc.) in NSCLC. Based on the UK Biobank dataset, the metabolite NAAG was identified as the most relevant to NSCLC and metabolomic analysis was conducted at the single-cell level. Additionally, an "inflammation-metabolism" network was constructed by integrating multi-omics analyses, including proteomics, transcriptomics, and metabolomics.

Multiple inflammatory proteins and metabolites were subsequently identified in NSCLC, which could potentially serve as therapeutic targets and prognostic biomarkers. The "inflammation-metabolism" network highlighted key miRNA-associated and protein-targeted pathways, as well as enriched signaling pathways related to NSCLC pathogenesis, laying the groundwork for subsequent epigenetic and functional analyses. Hence, these findings need to be validated through future translational and clinical practice.

2 Methods

The overall study design is presented in Fig. 1. Exposure data for 91 inflammatory proteins were obtained from Zhao et al.[21], while data for 731 immune cells were obtained from the study by Valeria Orrù et al. [22] and can be accessed in the Genome-Wide Association Studies Catalog (GCST0001391 to GCST0002121). Data related to 1,400 metabolites from Chen et al. were also included in the analysis [23]. Outcome data for NSCLC were obtained from the FinnGen database (ncases = 5315, ncontrol = 314,193), and validation data were acquired from the UK Biobank database for lung cancer (ncases = 2671, ncontrols = 372,016). These data were from populations of European ancestry. Genetic variants with strong associations with exposures/outcomes were selected as single nucleotide polymorphisms (SNPs). MR analyses for exposures (91 inflammatory proteins, 731 immune cells, and 1,400 metabolites) and outcomes (NSCLC) identified four inflammatory proteins, five immune cells, and seven metabolites potentially associated with NSCLC. After the MR analyses, PPI analysis, single-cell analysis, and multi-omics analysis were conducted: (1) PPI analysis of interactions for the relevant inflammatory proteins, with a focus on the four identified proteins, (2) single-cell analysis: the expression of the four inflammatory proteins, immune cells (effector memory CD4 + T cells and B cells), and metabolites (NAAG) in NSCLC, and (3) multi-omics analysis: Key nodes and enriched pathways in the "inflammation-metabolism" network in NSCLC.

2.1 Mendelian randomization analysis

The study was conducted in adherence with the core assumptions of MR (Supplementary Fig. 1), and the criteria for screening SNPs associated with inflammatory proteins, immune cells, metabolites, NSCLC, or lung cancer were: (1) Selection of SNPs strongly associated with inflammatory proteins ($p < 5 \times 10^{-6}$), immune cells ($p < 5 \times 10^{-6}$), metabolites ($p < 1 \times 10^{-5}$), NSCLC and lung cancer ($p < 5 \times 10^{-8}$). If there were duplicate SNPs within the same exposure, the SNP with the lowest P-value was further analyzed. (2) To ensure independence among SNPs, linkage disequilibrium (LD) clustering was performed with a filtering criterion of $r2 < 0.001$ within a 10,000 kb window [24]. This step ensured that the selected SNPs were not in significant LD with each other. (3) SNPs with a minor allele frequency (MAF) < 0.01 were excluded due to their limited reliability [25]. SNPs with excessively low MAF may reduce the statistical power and increase false-positive results.

To address potential weak instrument bias, the F-statistic for each SNP was calculated, and SNPs with an F-statistic < 10 were excluded, following established guidelines for instrument strength [26]. The F-statistic was calculated using the formula: $R2 = 2 \times EAF \times (1-EAF) \times beta2$; $F = R2 \times (N-2)/(1-R2)$ [26]. In the formula, EAF is the effect allele frequency, beta represents the effect size of the SNP, and N means the sample size. This rigorous screening process ensured that all included instrumental variables (IVs) were sufficiently strong to minimize bias in the causal estimates. The final instrumental variables (IVs) used are listed in Supplementary Tables 1B, 2B, and 3B.

For MR analysis, we systematically tested for potential violations of MR assumptions. The Q-statistic was utilized to assess the heterogeneity of the IVs [27], which can indicate the presence of pleiotropy when significantly elevated. Additionally, the intercept term from the MR-Egger regression was employed to specifically assess horizontal pleiotropy and its potential impact on the causal estimates [28]. Results with evidence of significant horizontal pleiotropy (MR-Egger intercept $p < 0.05$) were excluded to ensure the reliability of the MR estimates.

Discover Oncology (2025) 16:847 | https://doi.org/10.1007/s12672-025-02692-z

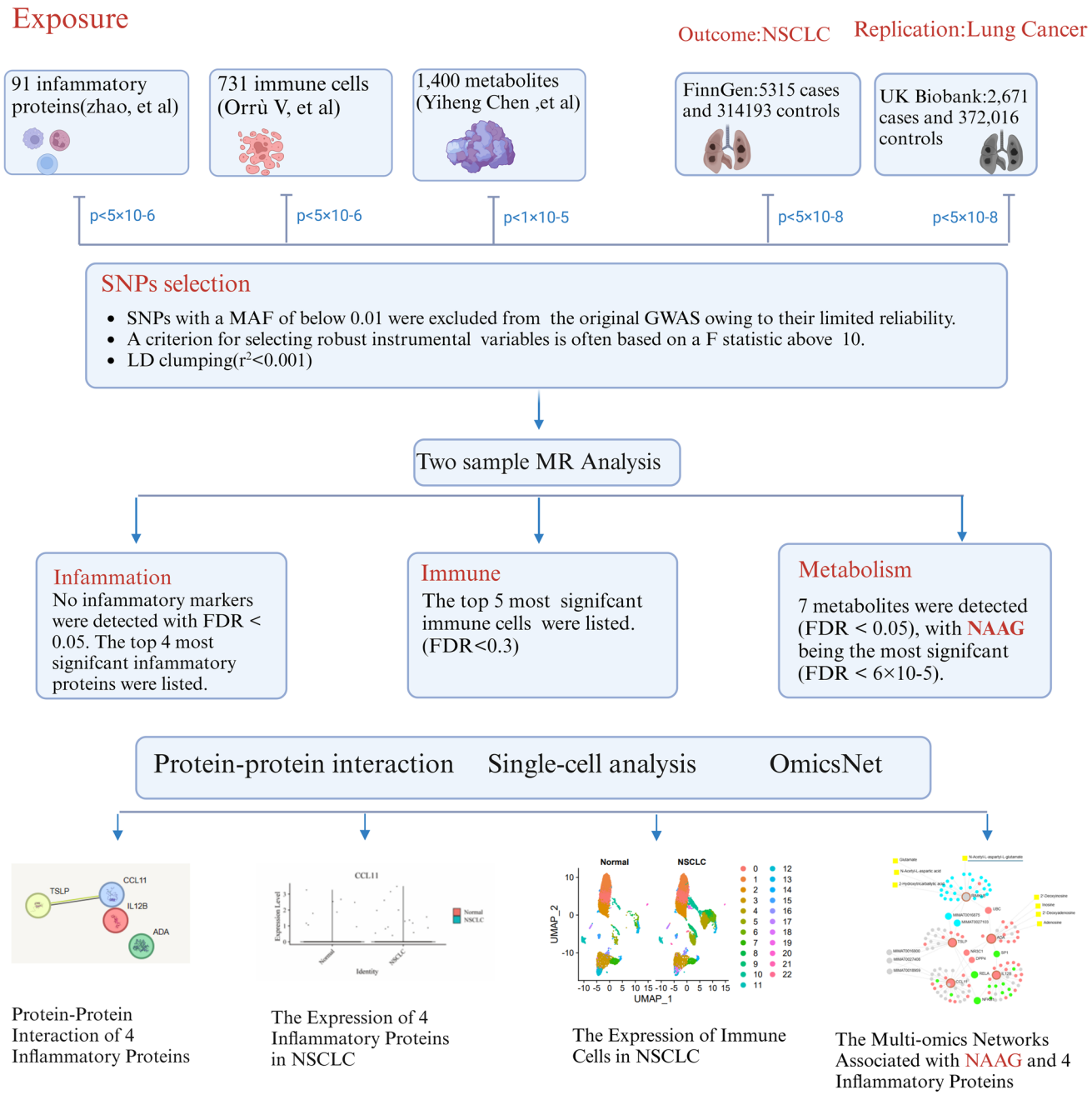

Fig. 1 Study workflow diagram. The diagram illustrates the research process (from top to bottom), including exposure and outcome-related information, criteria for SNP selection, and inflammatory proteins, immune factors, and metabolites associated with NSCLC identified through MR analysis. Based on these findings, PPI analysis, single-cell analysis, and multi-omics network analysis were performed. NAAG, N-acetyl-aspartyl-glutamate; NSCLC, non-small cell lung cancer; SNPs, single nucleotide polymorphisms; MR, Mendelian randomization; PPI, protein–protein interaction

The causal effect of SNPs on NSCLC was evaluated using multiple MR methods, including the simple mode, weighted mode, weighted median [29], MR-Egger, and inverse-variance weighted (IVW) method [30]. Among these, IVW weighs each estimate by its variance to reduce bias and is considered the primary and most robust method [31], particularly when no significant pleiotropy is detected. The consistency of results across different MR methods, which rely on different assumptions, further strengthened our confidence in the validity of the causal relationships identified.

The robustness of the results was assessed by performing leave-one-out sensitivity analyses. Each SNP was iteratively excluded, and the MR analysis was re-run to evaluate the impact of individual SNPs on the overall causal estimates, detect

outliers, and acquire guidance for the selection of IVs [32]. This approach helps identify potentially pleiotropic SNPs and improves the reliability and robustness of the MR analysis. The type I error rate in multiple testing was controlled using false discovery rate (FDR) correction; an FDR < 0.05 was considered significant. All analyses were conducted in R software (version 4.2.3).

2.2 Single-cell analysis and protein–protein interaction analysis

The single-cell RNA-seq data of NSCLC tissues and adjacent normal tissues were obtained from the Gene Expression Omnibus (GEO) database (GSE198099). We initially preprocessed the single-cell RNA-seq data using the "Seurat" [33] package, retaining cells with mitochondrial genes < 10%, total gene count > 200, and expression between 200 and 4000. Thus, low-quality cells and genes were filtered out through this step, which ensured data quality. After preprocessing, the gene expression levels of single cells were normalized using "LogNormalize" for comparable expression levels between different cells. Variable genes were identified though "FindVariableFeatures", while the influence of different gene expression levels was eliminated employing "ScaleData". Batch effects in the single-cell data was removed using "Harmony". For dimensionality reduction, RunPCA was conducted, and principal components were obtained. Unsupervised clustering analysis was performed using the "FindNeighbors" and "FindClusters" methods based on the co-occurrence clustering algorithm. These methods were selected to ensure accurate cell-type identification and robust downstream functional analysis of NAAG-related pathways in NSCLC.

Clustered cells were annotated according to cell type using the "SingleR" package[34] based on the reference dataset (HumanPrimaryCellAtlasData), and10 cell subtypes (T cells, B cells, etc.) were identified. After annotation, the distribution of different cell types was visualized in the low-dimensional space using UMAP. The expression of Effector Memory CD4 + T cells in NSCLC was further investigated by annotating and subdividing T cell subgroups into nine cell subtypes. To explore the activation and expression of the core metabolite NAAG in NSCLC, the Kyoto Encyclopedia of Genes and Genomes (KEGG) website was searched for core signaling pathways related to NAAG metabolism (https://www.genome.jp/kegg/) and gene sets associated with NAAG metabolism were retrieved from the MSIGDB website (https://www.gsea-msigdb.org/). The aim of these analyses was to investigate how NAAG metabolic pathways are activated across different immune cell populations in the tumor microenvironment.Single-cell expression analysis of these gene sets in NSCLC revealed NAAG-related activation states, metabolic activity, and receptor expression across different cellular subpopulations (Fig. 4A). Differentially expressed genes between high and low expressed-NAAG cell groups were identified using "FindMarkers" function in Seurat. Combined with GSEA, enrichment analysis was performed, and after multiple hypothesis correction, significantly enriched pathways with p-values < 0.25 were selected and represented by Fig. 4B.

We inferred high-confidence transcription factors associated with NAAG receptor expression by integrating the VIPER algorithm and the "DoRothEA" (Dysregulated Regulatory Element and Transcription Factor Activity) package and visualized them using a heatmap (Fig. 4C).

The communication network between cells was inferred employing "CellChat" package, "CreateNichConObject" and "TransCommuProfile" functions [35]. The pathway enrichment and strength of communication between these communication pairs were visualized through bubble plots (Fig. 4D) and circular plots (Fig. 4E). The analyses were conducted in R software (version 4.2.3).

The interactions between the target inflammatory proteins [36] was investigated by performing PPI analysis on the website (https://string-db.org/). The functions of the inflammatory proteins were explored by conducting protein function enrichment analysis using "genemania" (https://genemania.org/).

2.3 Multi-omics network analysis

Multi-omics analysis was performed using "OmicsNet2.0" (https://www.omicsnet.ca/) [37]. The input data comprised four inflammatory proteins and seven metabolites (some missing) associated with NSCLC, obtained from the MR analysis. The IDs for corresponding genes for the proteins were retrieved from the National Center for Biotechnology Information (NCBI) (https://www.ncbi.nlm.nih.gov/), and the information related to the NAAG gene was obtained from (https://www.genecards.org/). The "protein–protein" relationships were established based on the "InnateDB" database. The "miRNA-mRNA" relationships were established according to the "miRTarBase" database, and the "metabolite–protein" interactions were established based on the KEGG database. Finally, the "transcription factor-target gene" relationships were established based on the "TRRUST" database. The individual sub-networks were combined to construct a multi-omics network, which finally included 13 transcription factors, 8 metabolites, 27 miRNAs, 55 mRNAs/proteins, and 145 edges.

The multi-omics network was visualized in 2D and 3D employing "OmicsNet2.0". The focus was primarily on the interactions between NAAG and the four inflammatory proteins in the multi-omics network analysis. The "Function Explorer" provided by "OmicsNet2.0" was used to assess the enriched signaling pathways in this network.

2.4 Molecular docking

To explore the potential molecular interactions between key metabolites and inflammatory proteins identified in this study, molecular docking was performed as a predictive approach to assess binding affinity and interaction plausibility at the molecular level.

The 2D molecular structure of NAAG, a key metabolite identified in the MR analysis, was retrieved from the PubChem database (https://pubchem.ncbi.nlm.nih.gov/) in the SMILES format. The 3D structures of the target inflammatory protein were obtained from the UniProt database (https://www.uniprot.org/) and the RCSB Protein Data Bank (PDB; https://www.rcsb.org/), ensuring high-resolution and biologically relevant conformations were selected.

Molecular docking was conducted using the CB-Dock2 online server (http://clab.labshare.cn/cb-dock2/), which integrates cavity detection and AutoDock Vina-based docking to predict optimal binding modes. CB-Dock2 was selected due to its ability to automatically detect potential binding pockets and generate reliable docking scores without requiring manual predefinition of binding sites, making it suitable for ligand–protein interaction screening in exploratory studies.

Docking results were evaluated based on predicted binding energy values (in kcal/mol). A binding energy ≤ –5.0 kcal/mol is generally considered indicative of a strong binding affinity between the ligand and the receptor, suggesting a potentially meaningful interaction worthy of further investigation.

3 Results

3.1 Mendelian randomization analysis results

To enhance the interpretability of the results, we applied an evidence grading approach based on statistical thresholds and external validation: associations with *FDR* < 0.05 and replicated in an independent dataset were classified as Grade 1, those with *FDR* < 0.3 and nominal *P* < 0.05 as Grade 2, and associations with nominal *P* < 0.05 as Grade 3.

Among the 1,400 metabolites, seven were identified as causally associated with non-small cell lung cancer (NSCLC) under the condition of a false discovery rate (*FDR*) of less than 0.05 (Fig. 2B), and thus were considered Grade 2 evidence. Two metabolites were identified as protective factors for NSCLC, including N-acetyl-aspartyl-glutamate (NAAG; $\beta = -0.08$, 95% CI = −0.11 to −0.05, $P = 4.6 \times 10^{-8}$, $P_{FDR} = 0.0001$) and the ratio of oleoyl-linoleoyl-glycerol to linoleoyl-arachidonoyl-glycerol ($\beta = -0.13$, 95% CI = −0.20 to −0.07, $P = 7.64 \times 10^{-5}$, $P_{FDR} = 0.02$). Five metabolites were identified as risk factors for NSCLC, including the ratio of arachidonate to pyruvate ($\beta = 0.21$, 95% CI = 0.10 to 0.32, $P = 1.31 \times 10^{-5}$, $P_{FDR} = 0.03$), caffeine to paraxanthine ratio ($\beta = 0.28$, 95% CI = 0.14 to 0.93, $P = 1.13 \times 10^{-4}$, $P_{FDR} = 0.03$), 1-(1-enyl-palmitoyl)-2-arachidonoyl-glycerophosphocholine (GPC) levels ($\beta = 0.12$, 95% CI = 0.06 to 0.18, $P = 6.15 \times 10^{-5}$, $P_{FDR} = 0.02$), 1-stearoyl-2-arachidonoyl-GPC levels ($\beta = 0.11$, 95% CI = 0.06 to 0.19, $P = 5.89 \times 10^{-5}$, $P_{FDR} = 0.02$), and phenyllactate (PLA) levels in elite athletes ($\beta = 0.19$, 95% CI = 0.10 to 0.29, $P = 5.18 \times 10^{-5}$, $P_{FDR} = 0.02$) (Supplementary Table 3A). The F-statistic values for all instrumental variables (IVs) were > 10 (Supplementary Table 3B), and the MR-Egger intercept indicated no evidence of horizontal pleiotropy (Supplementary Table 3C). Results from simple mode, weighted mode, weighted median, and MR-Egger were all consistent with the inverse-variance weighted (IVW) method (Supplementary Fig. 2).

Among these metabolites, NAAG demonstrated a strong association with NSCLC in the UK Biobank validation dataset ($n_{case} = 2{,}671$, $n_{control} = 372{,}016$), with $\beta = -4.9 \times 10^{-4}$, 95% CI = -7.4×10^{-4} to -2.6×10^{-4}, $P = 5.5 \times 10^{-5}$, and $P_{FDR} = 0.08$ (Supplementary Table 4), and was therefore classified as Grade 1 evidence. The molecular structure of NAAG was obtained from PubChem (https://pubchem.ncbi.nlm.nih.gov/) and is shown in Fig. 2A.

At the threshold of *P* < 0.05, four inflammatory proteins were identified as Grade 3 evidence possibly associated with NSCLC (Fig. 2C). Among them, one was identified as a risk factor, namely eotaxin (CCL11; $\beta = 0.140$, 95% CI = 0.016 to 0.26, P* = 0.027), and three were identified as protective factors, including thymic stromal lymphopoietin (TSLP; $\beta = -0.175$, 95% CI = −0.337 to −0.013, P = 0.034), adenosine deaminase (ADA; $\beta = -0.175$, 95% CI = −0.337 to −0.013, P = 0.034), and interleukin-12B (IL-12B; $\beta = -0.081$, 95% CI = −0.160 to −0.003, P = 0.042) (Supplementary Table 1A). All MR methods produced consistent results (Supplementary Fig. 3), and F-statistics were > 10 with no horizontal pleiotropy (Supplementary Tables 1B and 1C).

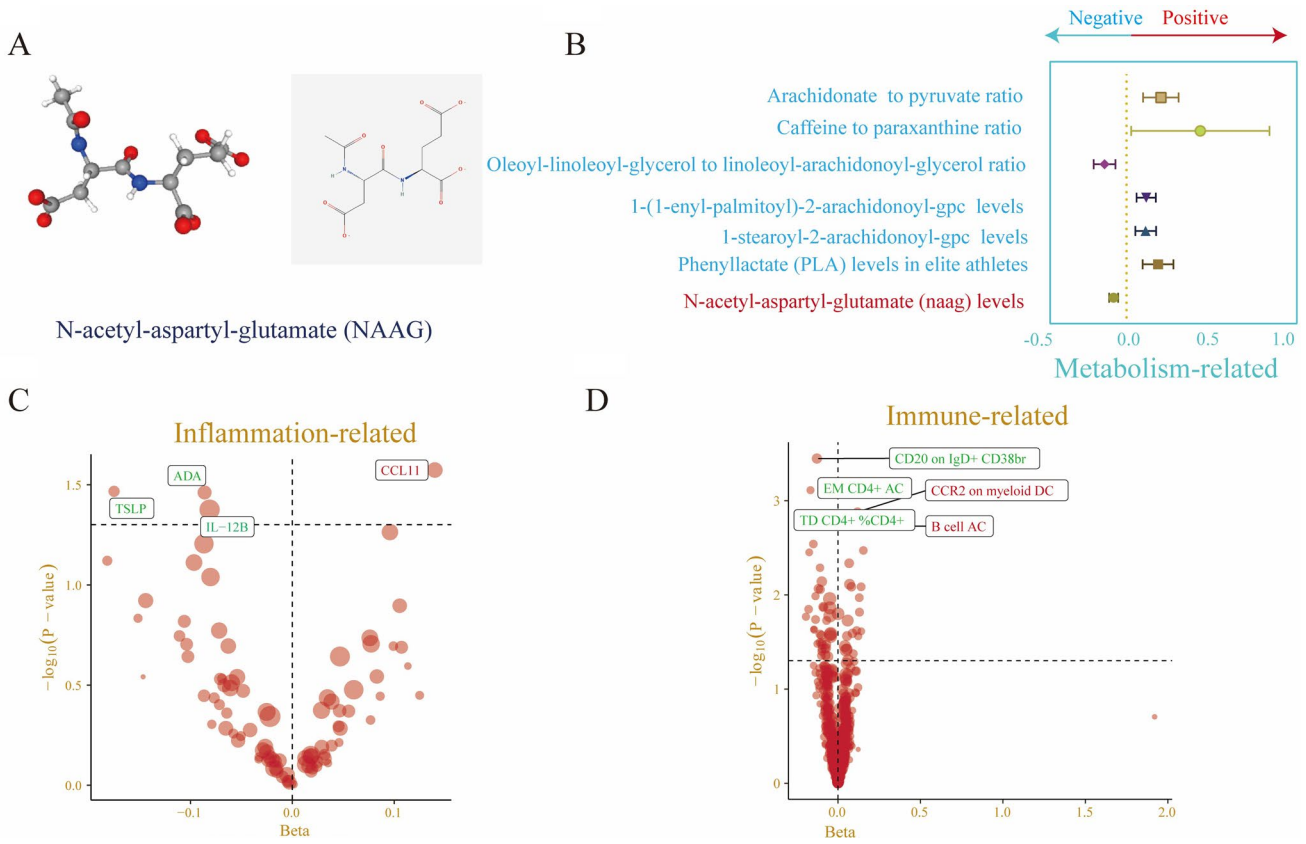

Fig. 2 The results of MR of inflammatory proteins, immune cells, and metabolites associated with NSCLC. **A** 2-dimensional (2D) and 3D chemical structure diagrams of NAAG. **B** MR analysis showing the effects (β estimates) of seven metabolites on NSCLC. **C** Volcano plot displaying four immune proteins associated with NSCLC ($p < 0.05$) identified through MR analysis. Red text indicates risk factors, while green text represents protective factors. **D** Volcano plot presenting five immune cell types associated with NSCLC identified through MR analysis. Red text denotes risk factors, and green text signifies protective factors. NSCLC, non-small cell lung cancer; NAAG, N-acetyl-aspartyl-glutamate; MR, Mendelian randomization

Under the threshold of $FDR < 0.3$ and $P < 0.05$, five immune cell types were identified as Grade 2 evidence possibly associated with NSCLC (Fig. 2D). Among them, three were protective factors, including CD20 on IgD^+ $CD38^{bright}$ cells ($\beta = -0.128$, 95% CI = −0.198 to −0.058, $P = 3.57 \times 10^{-4}$, $P_{FDR} = 0.26$), effector memory (EM) $CD4^+$ AC ($\beta = -0.167$, 95% CI = −0.264 to −0.070, $P = 0.001$, $P_{FDR} = 0.27$), and terminally differentiated (TD) $CD4^+$ $\%CD4^+$ ($\beta = -0.139$, 95% CI = −0.225 to −0.053, $P = 0.002$, $P_{FDR} = 0.27$). Two were identified as risk factors: B cell AC ($\beta = 0.131$, 95% CI = 0.048 to 0.213, $P = 0.002$, $P_{FDR} = 0.27$) and CCR2 on myeloid dendritic cells (DC) ($\beta = 0.118$, 95% CI = 0.046 to 0.190, $P = 0.001$, $P_{FDR} = 0.27$) (Supplementary Table 2A). The MR results were robust across multiple methods, including simple mode, weighted mode, weighted median, and MR-Egger (Supplementary Fig. 4). All IVs had F-statistics > 10 (Supplementary Table 2B), and no horizontal pleiotropy was observed (Supplementary Table 2C).

Leave-one-out analyses further demonstrated the robustness of the MR results for metabolites, inflammatory proteins, and immune cells in relation to NSCLC, reducing the risk of bias due to individual SNP outliers (Supplementary Figs. 5, 6, and 7).

3.2 Single-cell analysis and protein–protein interaction analysis results

3.2.1 Immune cells and non-small cell lung cancer

The expression and mechanisms of inflammatory proteins, immune cells, and metabolites in NSCLC was further investigated using the dataset GSE198099 from the GEO database. The differential expression of B cells in NSCLC and normal tissues was explored by performing first-level cell classification; 10 cell subtypes were identified (B cells, NK cells, T cells, monocytes, macrophages, DCs, endothelial cells, smooth muscle cells, and neutrophils) (Fig. 3A). Simultaneously, the

proportions of these 10 cell types in NSCLC and normal tissues were calculated (Fig. 3B). B cells were in a higher proportion in NSCLC tissues compared to normal tissues, consistent with the previous MR results indicating B cells as a risk factor for NSCLC. Building upon this, based on marker gene annotation, we subdivided the T cell subsets and identified nine T cell subtypes (effector memory CD4 + T cells, effector memory CD8 + T cells, naive CD4 + T cells, CD4 + Th17 cells, exhausted CD8 + T cells, CD4 + central memory T cells, CD4 + Tregs, and follicular helper CD4 + T cells) (Fig. 3C). The proportions of these T cell subsets in NSCLC and normal tissues were also calculated (Fig. 3D). Interestingly, effector memory CD4 + T cells were present in a higher proportion in normal tissues compared to NSCLC tissues, consistent with the previous MR results suggesting the protective role of effector memory CD4 + T cells in NSCLC.

3.2.2 Metabolites and non-small cell lung cancer

The expression patterns of NAAG activation, steady-state, metabolism are displayed in bubble plot (Fig. 4A), and receptor-related genes across different cell subpopulations in NSCLC are presented in Supplementary Table 5. The bubble plot reveals that NAAG is more readily activated in T cells and NK cells, while monocytes and macrophages presented with higher levels of NAAG-related metabolic activity. Thus, NAAG may play distinct roles in regulating immune cell functions versus metabolic processes in the TME.

In NSCLC, NAAG influences pathways of inflammation, immunity, and protein synthesis, such as the B cell receptor signaling pathway, acute inflammatory response to antigen stimulus pathway, and positive regulation of the protein oligomerization pathway (Fig. 4B). The potential role of NAAG in modulating B cell activation, antigen-induced

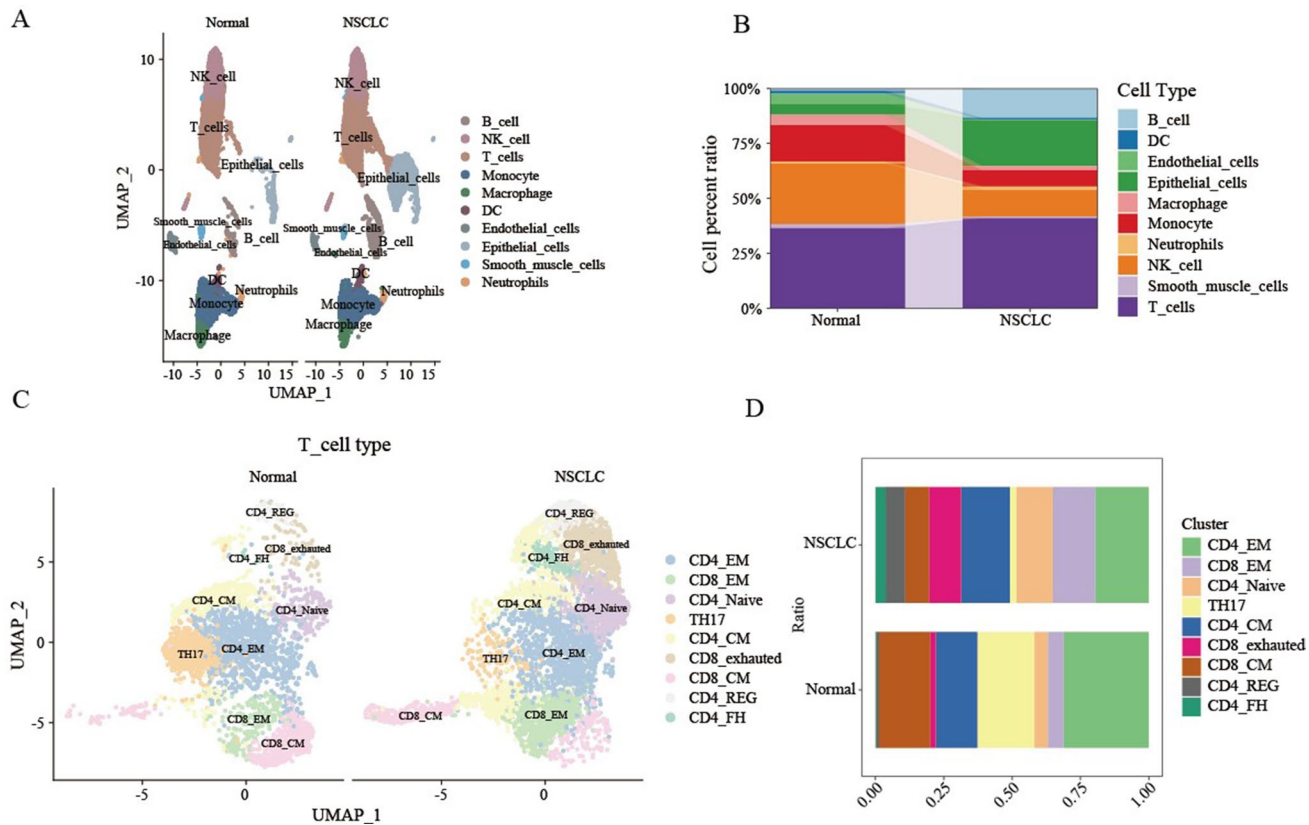

Fig. 3 The results of single-cell analysis of immune cells in NSCLC. **A** Ten cell subtypes were identified in the first round of clustering, including B cells, NK cells, T cells, monocytes, macrophages, DCs, endothelial cells, smooth muscle cells, and neutrophils. **B** The proportions of the 10 cell subtypes in normal and NSCLC tissues. **C** The second round of clustering identified nine T cell subtype. **D** The proportions of the nine T cell subtypes in normal and NSCLC tissues. NSCLC, non-small cell lung cancer; NK cells, natural killer cells; DCs, dendritic cells; CD4_EM, effector memory CD4 + T cells; CD8_EM, effector memory CD8 + T cells; CD4_Naive, naive CD4 + T cells; Th17, CD4 + T helper type 17 cells; CD8_exhausted, exhausted CD8 + T cells; CD4_CM, CD4 + central memory T cells; CD4_REG, CD4 + regulatory T cells; CD4_FH, CD4 + T follicular helper cells

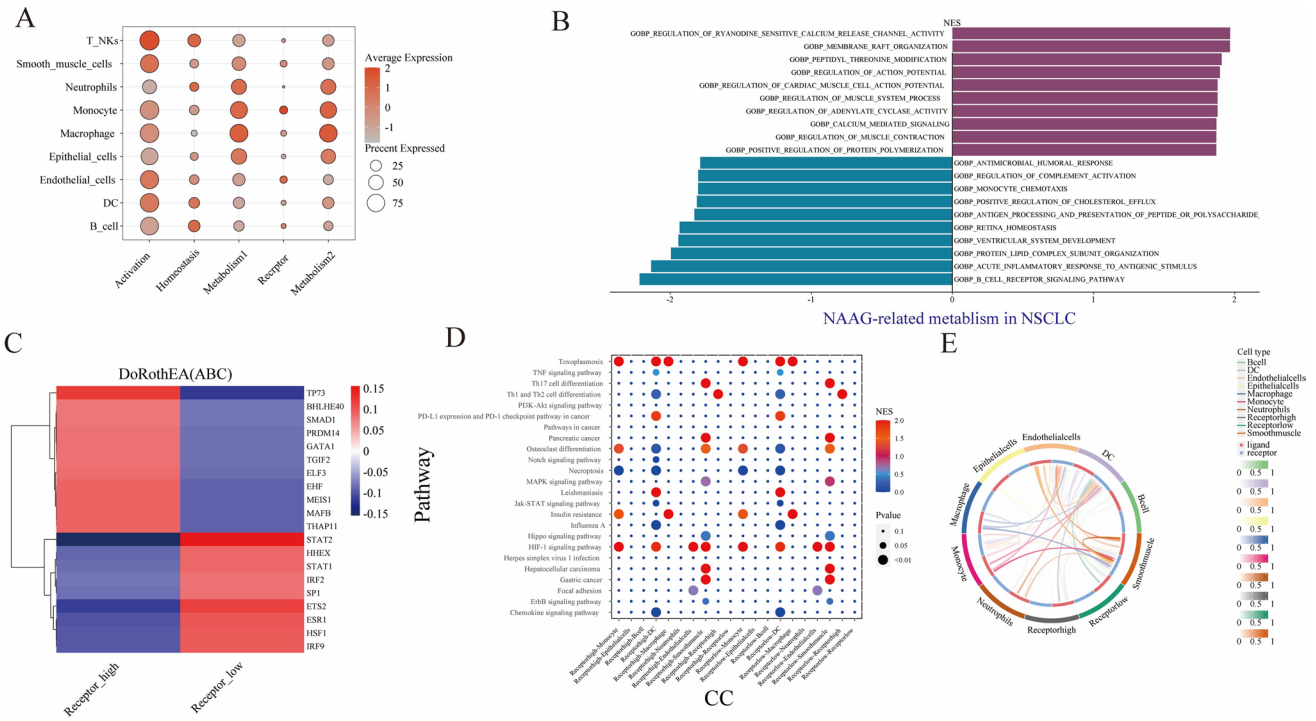

Fig. 4 The expression of NAAG, enriched pathways, regulatory transcription factors, and cell communication in NSCLC. **A** Bubble plot showing the expression of genes related to NAAG activation, homeostasis, metabolism, and receptors across cell subpopulations of NSCLC. **B** Heatmap illustrating the impact of NAAG on the expression of metabolic pathways in NSCLC. Purple represents upregulated pathways, while green represents downregulated pathways. **C** Heatmap depicting the influence of high and low NAAG receptor expression on the expression of transcription factors. **D** Comparative analysis of the impact of high and low expression of NAAG receptor on enriched pathways in different cell subpopulations. **E** Cell communication network in NSCLC cell subpopulations. The outer circle represents different cell types, with each color corresponding to a specific cell type. In the inner circle, ligands are presented in red and receptors in blue. The inner and outer circles are connected by lines, which represent cell–cell communication. NSCLC, non-small cell lung cancer; NAAG, *N*-acetyl-aspartyl-glutamate

inflammatory responses, and regulation of protein complexes is evidenced through the enrichment of these specific pathways.

The transcription factor activity heatmap (Fig. 4C) demonstrates the function of NAAG in upregulating the transcriptional activity of the tumor suppressor gene TP73. TP73 can suppress uncontrolled cell proliferation by inducing a series of defense mechanisms, including DNA repair, apoptosis, and cell cycle regulation [38]. Notably, in NSCLC, mutations in TP53 correlate with poorer prognosis [39, 40]. Interestingly, the combination of Nutlin-3 (an MDM2 inhibitor activating p53) and cisplatin in NSCLC cells can induce p53-dependent apoptosis, thereby suppressing tumor progression [41]. NAAG expression is also associated with the downregulation of the inflammation-related transcription factor, signal transducer and activator of transcription 1 (STAT1), which is implicated in driving tumor invasion, progression [42], and in the reprogramming of glucose metabolism in lung adenocarcinoma (LUAD), contributing to LUAD progression [43].

The signaling pathway (Fig. 4D) reveals that different levels of NAAG expression can lead to variations in the expression of the Notch signaling pathway; higher levels of NAAG results in the downregulation of Notch signaling pathway. The Notch signaling pathway plays a pivotal role in the development of lung cancer, and interacts with various transcription factors such as Snail, Slug, and TGF-β to promote epithelial-mesenchymal transition (EMT), thereby driving the progression of NSCLC [44]. The Notch pathway is also involved in regulating cell proliferation, stemness, and drug resistance in NSCLC [45]. Notably, the Notch inhibitory ligand Delta-like protein 3 (DLL3) showed a significant efficacy and safety in the treatment of lung cancer [46], highlighting the potential of targeting the Notch pathway in NSCLC treatment.

The cell signaling pathway (Fig. 4E) demonstrates ligand-receptor interactions among endothelial cells, macrophages, smooth muscle cells, and DCs, respectively influencing angiogenesis, promoting tumor progression, regulating tumor vascularization, and modulating immune responses. Through these ligand-receptor signaling cascades, they exert cross-talk effects within the TME, playing crucial roles in the progression of NSCLC.

3.2.3 Inflammation proteins and non-small cell lung cancer

To further investigate the relationship between inflammatory proteins and NSCLC, we selected 17 NSCLC-related proteins with the smallest to largest p-values in MR for analysis using the "string" tool. The PPI network analysis showed the location of the key "CCL2-CCL11-CCL13" triangle at the core of the network, suggesting that the primary biological functions of CCL11 were cytokine receptor binding, cytokine binding, and cytokine migration (Fig. 5A). CCL11 binds mainly to the CCR3 receptor to regulate eosinophils and Th2 cell chemotaxis [47]. Particularly, both CCL11 and TSLP can mediate the influence of eosinophils on the TME, leading to pro-tumor or anti-tumor effects [48]. Chemokines, including CCL2 and CCL11 are expressed at elevated levels in the airways and participate in pathological processes such as airway inflammation [49], remodeling, and hyperresponsiveness [50, 51].

Single-cell analysis revealed greater abundance of IL12B in DCs, TSLP was more abundant in epithelial cells, and CCL11 was primarily distributed in smooth muscle cells. Smooth muscle cells in the lungs are mainly distributed in the bronchioles, alveolar ducts, and small blood vessels; their contraction and migration affect gas exchange and blood supply. CCL2 can mediate fibroblast migration in airway smooth muscle (ASM) and promote ASM proliferation, leading to bronchial wall thickening [52]. CCL11 is an effective chemoattractant for vascular smooth muscle and can influence its migration [53]. ADA was relatively high in various cell types (T cells, NK cells, B cells, epithelial cells, and monocytes) (Fig. 5B). Additionally, CCL11 expression levels were higher in NSCLC compared to normal tissues, confirming the previous MR finding (CCL11 is a risk factor for NSCLC). In contrast, IL12B expression was higher in normal tissues compared to NSCLC tissues, confirming the previous MR analysis result, that IL12B is a protective factor against NSCLC (Fig. 5C).

The study findings provide valuable insights into the intricate interplay between inflammatory proteins and NSCLC. The identification of the "CCL2-CCL11-CCL13" axis as a core component of the PPI network suggests the importance

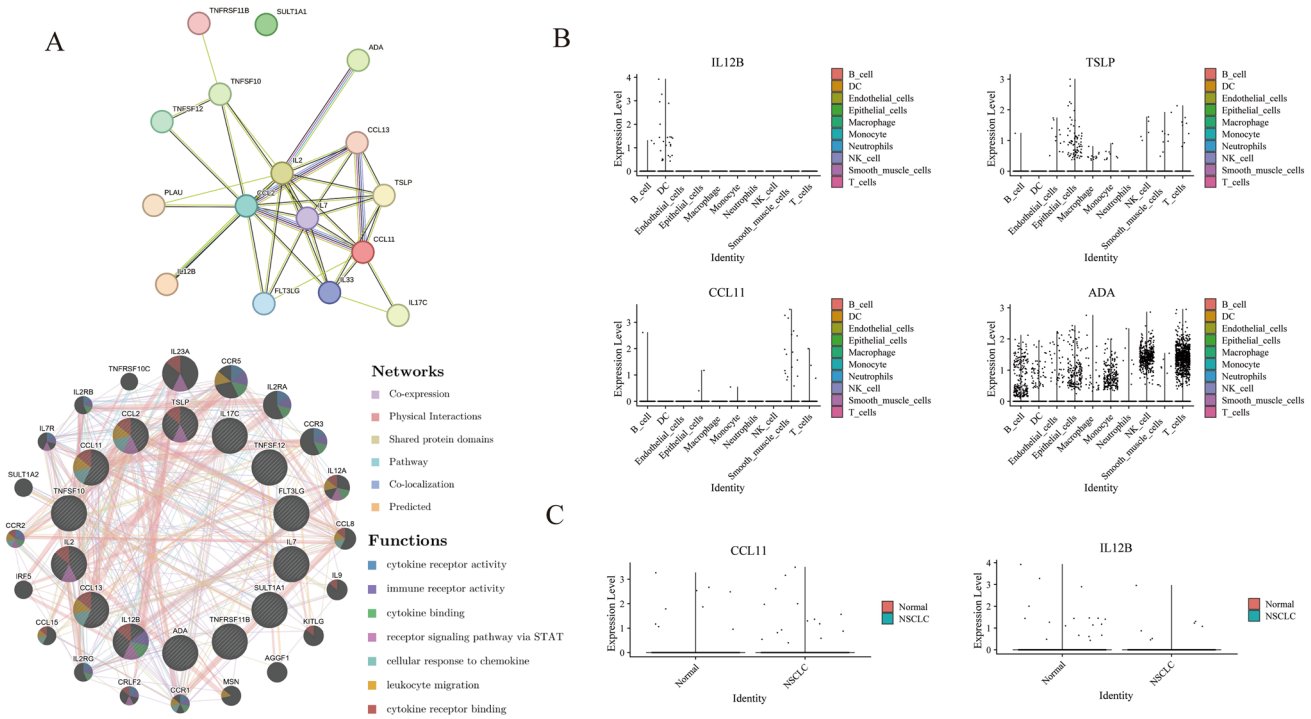

Fig. 5 Analysis of NSCLC-associated inflammatory proteins using PPI and single-cell analysis. **A** PPI network of 17 proteins. The upper panel shows the interactions between proteins, while the lower panel displays the interactions as well as biological functions of the proteins. Different colors of the lines represent different types of interactions between proteins (such as co-expression, physical interactions, etc.). Within each circle for a protein, different colors represent different biological functions such as cytokine receptor activity, immune receptor activity, etc. **B** Distribution of IL12B, TSLP, CCL11, and ADA across different NSCLC tissue subtypes (B cells, DCs, endothelial cells, epithelial cells, macrophages, monocytes, neutrophils, NK cells, smooth muscle cells, and T lymphocytes). **C** Comparison of the distribution of IL12B and CCL11 in normal and NSCLC tissues. The average IL12B expression was around 4.8-fold higher in normal tissues compared to NSCLC tissues. Conversely, the average CCL11 expression was approximately 1.2-fold higher in NSCLC tissues relative to normal tissues. NSCLC, non-small cell lung cancer; DCs, dendritic cells; NK cells, natural killer cells; PPI, protein–protein interaction; IL12B, interleukin 12B; TSLP, thymic stromal lymphopoietin; CCL11, C–C motif chemokine ligand 11; ADA, adenosine deaminase

of these chemokines in NSCLC pathogenesis. The differential expression of CCL11 and IL12B in NSCLC and normal tissues further supports their respective roles as risk and protective factors. The involvement of CCL11 and CCL2 in airway remodeling and smooth muscle migration suggests potential mechanisms by which these chemokines may contribute to the development and progression of NSCLC.

However, TME is a complex and dynamic system, and the effects of inflammatory proteins may vary according to the context and stage of the disease. Further research is needed to elucidate the precise mechanisms through which these proteins influence NSCLC development and progression and explore their potential as therapeutic targets or biomarkers.

3.3 Multi-omics network analysis results

Based on metabolic network analysis results, RIMKLB was identified as a key node linking NAAG with inflammatory proteins (ADA and TSLP), while miRNAs MIMAT0027103 and MIMAT0016875 were key nodes connecting NAAG with TSLP. Ubiquitin-conjugating enzyme E2 C (UBC) emerged as a crucial node between NAAG and ADA. Furthermore, ADA was found to regulate four related metabolites (Fig. 6A). The 3D conformational structurers further elucidated the relationships across different metabolomic levels, underscoring the roles of RIMKLB, ADA, TSLP, CCL11, and IL-12B at the nodes (Fig. 6B). KEGG pathway analysis identified the three most relevant pathways co-expressed across multiple nodes: (1) the Forkhead box O signaling pathway, which regulates cell cycle, metabolism, and cancer progression (involving 12 nodes); (2) the Th17 cell differentiation pathway, which regulates the differentiation of CD4 + T cells into Th17 cells (involving 10 nodes), and (3) the primary immunodeficiency pathway (involving seven nodes) (Supplementary Table 6).

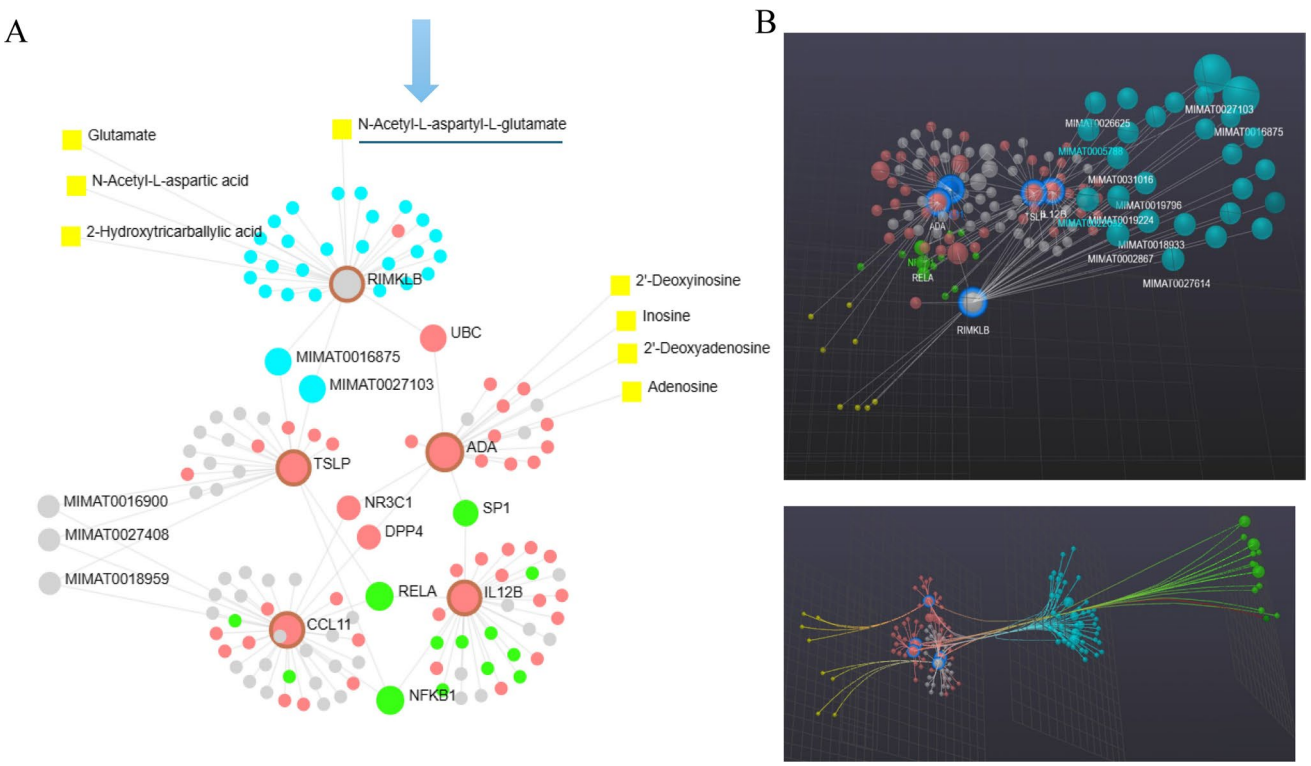

Fig. 6 Multi-omics analysis revealing the "inflammation-metabolism" network in NSCLC. **A** The multi-omics network focused on the relationships between NAAG and four inflammatory proteins. Gray nodes, mRNAs; blue nodes, miRNAs; yellow nodes, metabolites; red nodes, proteins; green nodes, transcription factors. The network comprises 13 transcription factors, 8 metabolites, 27 miRNAs, 55 mRNAs/proteins, and a total of 145 edges showing the interactions between "transcription factor-miRNA-mRNA/protein-metabolite". **B** A 3-dimensional representation of the multi-omics network, divided into four layers: the metabolome layer (yellow), the mRNA/proteome layer (gray and red), the miRNA layer (blue), and the transcriptome layer (green). This is a more intuitive representation of the crosstalk between different layers (e.g., metabolome, proteome) and their influence on other layers. NSCLC, non-small cell lung cancer; NAAG, *N*-acetyl-aspartyl-glutamate; mRNA, messenger RNA; miRNA, microRNA

3.4 Molecular docking results

The molecular docking analysis revealed that NAAG exhibited a binding energy of − 6.9 kcal/mol with adenosine deaminase (ADA), indicating a relatively strong binding affinity between the two molecules (Supplementary Fig. 8). This suggests that NAAG may participate in inflammation regulation through direct interaction with ADA.

4 Discussion

We performed MR analysis on two large cohorts and found a potential role of NAAG for NSCLC. NAAG is a neuronal metabolite, primarily in the context of the central nervous system. An increasing number of studies in recent years have reported the roles of NAAG in cancer, including its involvement in energy storage [54], metabolic cycling [55], and a potential therapeutic target [56, 57]. These mostly involved studies on ovarian cancer, glioma, prostate cancer, etc. [58, 59]. Currently, there is a lack of research on the role of NAAG in NSCLC. To our knowledge, this is the first study to examine the relationship between NAAG and NSCLC employing multi-omics approaches. To this effect, the present study illuminates following potential mechanisms by which NAAG exerts an inhibitory effect: (1) promoting the tumor suppressor TP53 expression, thereby preventing excessive cellular proliferation; (2) suppressing STAT1 and the Notch signaling pathway expression, as STAT1-mediated glucose reprogramming and Notch-driven EMT and 2chemotherapeutic resistance are known to facilitate the progression of NSCLC [42] (Fig. 7). In addition, NAAG also plays a significant role in suppressing

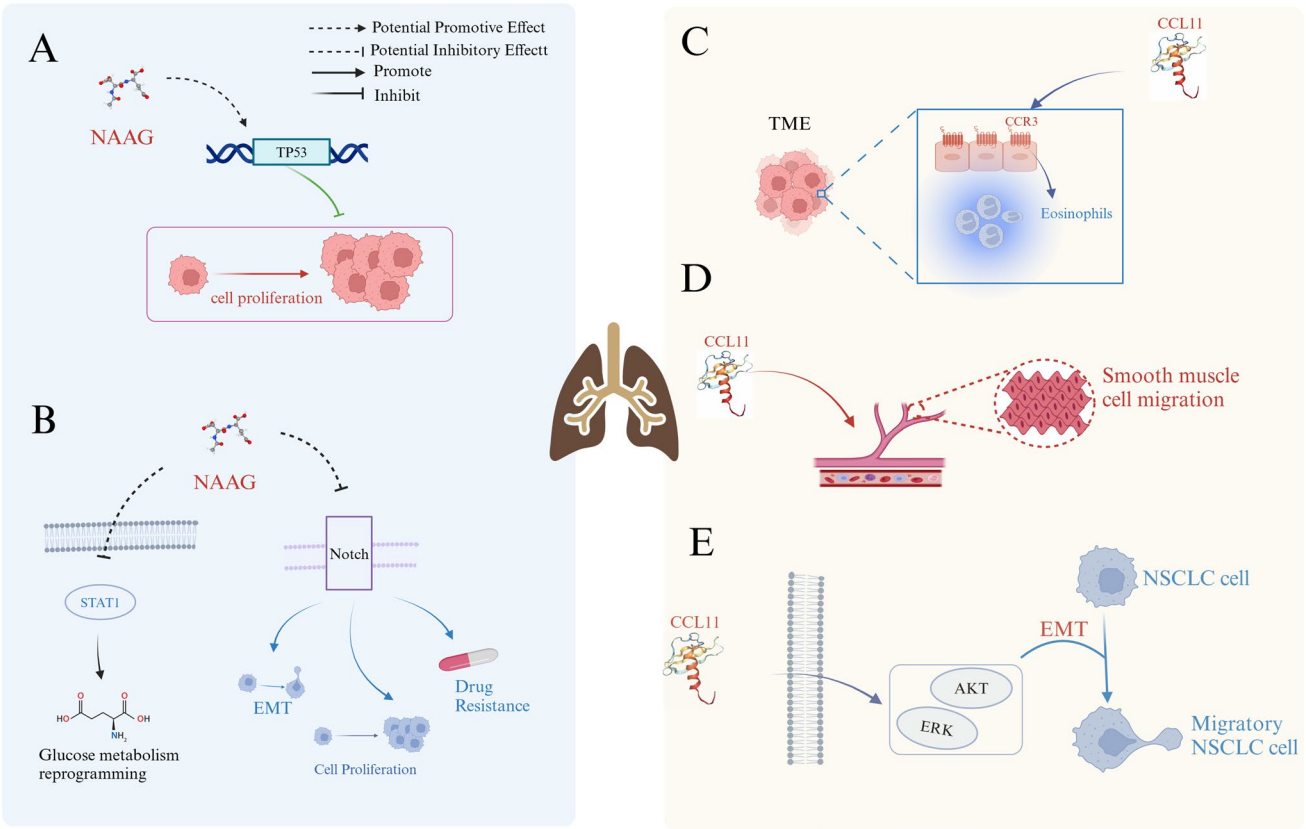

Fig.7 Mechanisms of action of NAAG (left) and CCL11 (right) in NSCLC/tumor-related processes. **A** NAAG upregulates TP53 expression, inhibiting cell proliferation. **B** NAAG inhibits the STAT1 pathway, suppressing glucose metabolic reprogramming and inhibiting LUAD; NAAG inhibits the Notch pathway, suppressing EMT, cell proliferation, and drug resistance in NSCLC. **C** CCL11 promotes eosinophil infiltration in the tumor microenvironment (TME). **D** CCL11 promotes vascular smooth muscle cell migration. **E** CCL11 activates ERK and AKT, promoting EMT in NSCLC. NAAG, N-acetyl-aspartyl-glutamate; CCL11, C–C motif chemokine ligand 11; NSCLC, non-small cell lung cancer; TP53, tumor protein p53; LUAD, lung adenocarcinoma; EMT, epithelial–mesenchymal transition; TME, tumor microenvironment; ERK, extracellular signal-regulated kinase; AKT, protein kinase B

inflammation, which may further contribute to its anti-tumor effects [60, 61]. Subsequent studies building upon these findings might further delineate the mechanisms through which NAAG modulates NSCLC pathogenesis, potentially unveiling novel therapeutic avenues.

Our multi-omics network analysis linked NAAG with four inflammatory proteins (Fig. 4). In the "inflammation-metabolism" network, UBC was a key node linking NAAG and ADA; in fact, current studies also support that UBC may be a novel therapeutic target for lung cancer [62]. In NSCLC, UBC is involved in the regulation of apoptosis, tumor growth, and angiogenesis. UBC can regulate the phosphorylation levels of extracellular signal-regulated kinases 1 and 2 in NSCLC, thereby regulating apoptosis and increasing the expression levels of cell cycle protein D1 and matrix metalloproteinase-2 [63, 64]. Additionally, the 12 nodes in the "inflammation-metabolism" network collectively point to the FOXO signaling pathway. FOXO1 is a member of the FOXO family that is present mainly in the cytoplasm of NSCLC cells. FOXO1 in NSCLC is regulated by multiple signaling pathways; numerous studies have reported the role of FOXO1 in NSCLC suppression. In lung adenocarcinoma cells, c-Jun N-terminal kinases positively regulates FOXO1, promoting its nuclear translocation. In response to repair DNA damage, nuclear FOXO1 can upregulate the expression of p27(Kip1), Bim, and GADD45 genes [65]. ROS, including superoxide anion (O^{2-}) and hydrogen peroxide (H_2O_2), can damage cellular nucleic acids and proteins, leading to cellular dysfunction. Excessive ROS accumulation can enhance FOXO1 expression by inhibiting the phosphoinositide 3-kinase/protein kinase B(PI3K/AKT) pathway, stimulating apoptosis and G2/M arrest in NSCLC cells [66]. Restored FOXO1 expression can also increase sensitivity to chemotherapy drugs, such as docetaxel, gefitinib, or cisplatin [67, 68].

The "metabolism-immune" module indicated that NAAG may interfere with the B cell receptor signaling pathway, suggesting a potential downregulation of B cell activity (Fig. 4B), suggesting that NAAG could lead to the downregulation of B cells (Fig. 4B). MR analysis indicated absolute B cell count as a risk factor for NSCLC (Fig. 2D), and single-cell analysis showed a significantly higher proportion of B cells in NSCLC tissues than in normal tissues (Fig. 3B). Therefore, we hypothesize that the inhibitory effect of NAAG on NSCLC may be achieved through downregulating B cells, although further experimental validation is needed to confirm this.To provide a comprehensive view of these cross-domain interactions, we have illustrated the metabolite–inflammation–immune interaction network in Supplementary Fig. 9.

Considering the inflammatory proteins, CCL11 was identified as a risk factor for NSCLC, while ADA, TSLP, and IL-12B emerged as protective factors (Fig. 2C). Further PPI analysis highlighted CCL11 as a key node (Fig. 5A), and this was corroborated by single-cell analysis verifying its elevated expression in NSCLC relative to normal tissues (Fig. 5C). Previous research was predominantly focused on the relationship between CCL11 and other cancers. For instance, in head and neck tumors, cancer-associated fibroblasts promote EMT and tumor invasion through CCL11 secretion [69]. In liver cancer, CCL11 activation of the CCR3 receptor augments vascular endothelial growth factor expression, fostering angiogenesis [70]. However, investigations into the role of CCL11 in NSCLC remain limited. The study by Lin et al. [71] demonstrated that CCL11 activates the AKT and ERK signaling pathways, facilitating NSCLC metastasis through the EMT, and high CCL11 expression is associated with lung cancer and poor prognosis, consistent with the current findings. CCL11 has been implicated in promoting metastasis of various lung cancers. Bekaert S et al. [72] demonstrated that allergen-induced allergic inflammation can facilitate breast cancer metastasis to the lungs through the CCL11-CCR3 axis, highlighting the potential role of CCL11 in creating a favorable microenvironment for the colonization and growth of tumor cells in the lungs.

Furthermore, the impact of CCL11 on the TME should be carefully considered. CCL11 has been shown to induce the infiltration of eosinophils into the TME [48]. Eosinophils secrete various growth factors and cytokines that can promote tumor growth and angiogenesis. CCL11 has also been reported to mediate vascular smooth muscle cell migration, potentially contributing to tumor angiogenesis [53]. CCL11-mediated recruitment of eosinophils and the stimulation of vascular smooth muscle cell migration could create a supportive microenvironment for tumor growth and metastasis.

Evidence suggests that patients with lung cancer demonstrate reduced adenosine deaminase (ADA) activity in lymphocytes. This decrease may enhance the tumor-promoting effects of adenosine by elevating levels of interleukin-6 (IL-6) and tumor necrosis factor-alpha (TNF-α) while concurrently decreasing serum levels of interleukin-17 (IL-17) and interferon-gamma (IFN-γ) [73], thereby corroborating the aforementioned findings. The role of TSLP in cancer promotion or inhibition remains debatable, as it exhibits a promoting role in some cancers (ovarian, pancreatic, or gastric) but an inhibitory role in others (colon, skin) [74]. In lung adenocarcinoma, TSLP exerts an inhibitory effect, and its overexpression arrests LUAD cells in the G2/M phase, thus reducing viability, promoting apoptosis, and inhibiting cell migration and invasion [75], aligning with the research conclusions.

Considering the immune cells, the study focused on two immune cell types associated with NSCLC. The effector memory CD4 + T cells emerged as a protective for NSCLC, while B cells were identified as a risk factor (Fig. 2D). Effector memory CD4 + T cells are associated with immune response activation occurring in peripheral lymphoid organs.

Currently, research investigating the relationship between effector memory CD4 + T cells and NSCLC is lacking. Osamu Wakabayashi et al. [76] found the association of higher levels of CD4 + T cells in the NSCLC stroma with prolonged survival in patients with NSCLC. Iwona Kwiecień et al. [77] demonstrated a higher abundance of effector memory CD4 + T cells in metastatic lymph nodes compared to non-metastatic lymph nodes in lung cancer. Nonetheless, neither study specifically addressed the relationship between effector memory CD4 + T cells and NSCLC, indicating a need for further exploration. The role of B cells in NSCLC remains to be studied more extensively. Mouse experiments suggest that B cell-mediated inflammation may be crucial in promoting invasive malignant tumor progression [78]. Some studies propose that plasma-like B cells promote cell growth in late-stage non-small cell lung cancer (NSCLC) [79], In contrast, the favorable prognostic role of CD20 + B cells in NSCLC is frequently emphasized [80], and the presence of peritumoral B lymphocytes is closely associated with improved survival rates [81]. Therefore, one needs to be cautious when interpreting the study's findings regarding B cells, and further stratified research may be conducted to elucidate their relationship with NSCLC.

The strength of this study is the use of large-scale MR analysis to systematically assess the causal relationships between inflammation, immunity, and metabolism in NSCLC. The study design features a large sample size, wider coverage, and minimal bias. The research explored the role of inflammatory proteins, immune cells, and metabolites at the single-cell level in NSCLC. It analyzed their interactions and integrated multi-omics data to construct an "inflammation-immune-metabolism" network, providing multi-faceted insights into the mechanisms underlying NSCLC development. The multi-omics analysis conducted in this study demonstrated a protective role of NAAG and suggested a potential role of CCL11 as a risk factor for NSCLC. NAAG could exert its NSCLC inhibitory effects by promoting TP53 expression to prevent excessive cell proliferation, downregulate STAT1 and Notch signaling to suppress glucose reprogramming, EMT, and chemoresistance (Fig. 7). Future studies should explore the feasibility of NAAG as a biomarker for early NSCLC diagnosis and enhance NAAG expression or administer exogenous analogues as adjuvant therapies. Conversely, elevated CCL11 expression may correlate with poor prognosis. The prognostic value of CCL11 can be evaluated through analysis of the associations between CCL11 levels and clinicopathological features/survival, facilitating precise stratification and personalized treatment of NSCLC. Simultaneously, developing antagonists or inhibitors against the CCL11-CCR3 axis, in combination with anti-angiogenic therapies or immunomodulatory strategies, could be novel treatment options for patients with advanced or metastatic NSCLC. Furthermore, the influence of CCL11 on eosinophil infiltration in the ME and its role in tumor angiogenesis mediated by vascular smooth muscle cell migration need to be further investigated.

In summary, this study provides potential novel biomarkers and targets for NSCLC diagnosis, prognosis, and treatment. However, further in-depth research and validation studies are required for translating these findings into clinical applications.

Our study also has several limitations. First, the current analysis is limited to European populations, necessitating large-scale, multi-center clinical trials across diverse ethnic groups and regions to validate the generalizability and effectiveness of the findings. Although both the FinnGen and UK Biobank cohorts are composed predominantly of individuals of European descent, demographic and clinical heterogeneity between these cohorts may still influence the study outcomes. For instance, differences in smoking prevalence, environmental exposures, and the burden of comorbidities (such as chronic obstructive pulmonary disease or cardiovascular disease) could potentially confound the associations observed in MR analyses. While MR studies are generally less susceptible to confounding due to the random allocation of genetic variants at conception, residual confounding from unmeasured or cohort-specific factors cannot be entirely excluded. Moreover, differences in case definition or disease ascertainment between FinnGen and UK Biobank may also contribute to heterogeneity in effect estimates. To mitigate these issues, we limited our analyses to populations of European ancestry and used separate cohorts for discovery (FinnGen) and replication (UK Biobank), which enhances the robustness and reproducibility of our findings.

Second, in the immune cell analysis, evidence supporting the association between effector memory CD4 + T cells and NSCLC is lacking; the role of B cells may require further subtyping to examine the differential impacts of distinct B cell subpopulations. Although MR analysis in this study did not identify CCL2 as a risk factor for NSCLC, subsequent PPI analysis identified a strong interaction between CCL11 and CCL2; in fact, existing literature supports the role of CCL2 in promoting airway inflammation and remodeling, warranting further investigation into its contributory role in NSCLC progression. Moreover, mechanistically, the link between NAAG and NSCLC remains largely unexplored; while this study provides potential research directions, experimental validation remains crucial. Finally, due to limitations in the available databases, it was not possible to construct a comprehensive "inflammation–immune–metabolism" network. Consequently, additional clinical studies are needed to investigate key nodes within this network and to develop a more comprehensive multi-omics model. Overall, although there are some limitations, this study could construct an NSCLC-related

"inflammation–immunity–metabolism" network, uncover key pathways and nodes, deepen the understanding of NSCLC-associated pathogenic mechanisms, and provide valuable insights for discovering new therapeutic targets.

5 Conclusions

In this study, several inflammatory proteins, immune cells, and metabolites associated with NSCLC risk were identified to provide novel insights into the etiology of NSCLC. We further uncovered key pathways and targets by constructing an "inflammation–immunity–metabolism" network related to NSCLC. These findings offer promising candidates to develop screening biomarkers and therapeutic targets for NSCLC. Nonetheless, further experimental and clinical investigations are warranted to evaluate and validate the utility and efficacy of these candidates.

Acknowledgements We would like to express our gratitude to the FinnGen database for providing the data, and to the editors and reviewers for their helpful comments on the manuscript.

Author contributions J.Q.Z.: Writing—original draft, Writing—review and editing; L.P.L.: Writing—original draft; W.Y.L.: Writing—review; J.G.: Writing—review and editing. All authors reviewed the manuscript.

Funding The authors declare financial support was received for the research, authorship, and publication of this article. This work was supported in part by grants from the National Natural Science Foundation of China Youth Fund (No. 82305188), the Sichuan Provincial Natural Science Foundation Youth Fund (No. 23NSFSC6246), and the China Postdoctoral Science Foundation (No. 2022MD723715).

Data availability The datasets presented in this study can be found in online repositories. The FinnGen database data are available at https://www.finngen.fi/en/access_results. and the GWAS summary datasets are available at https://gwas.mrcieu.ac.uk/.

Declarations

Ethics approval and consent to participate For this study, no additional informed consent or ethics approval is required, as all data is derived from previously published resources and informed consent and approval had already been obtained.

Competing interests The authors declare no competing interests.

References

1. Siegel R, Ma J, Zou Z, Jemal A. Cancer statistics, 2014. CA Cancer J Clin. 2014;64(1):9–29.
2. Thomas SJ, Snowden JA, Zeidler MP, Danson SJ. The role of JAK/STAT signalling in the pathogenesis, prognosis and treatment of solid tumours. Br J Cancer. 2015;113(3):365–71.
3. Tan Z, Xue H, Sun Y, Zhang C, Song Y, Qi Y. The role of tumor inflammatory microenvironment in lung cancer. Front Pharmacol. 2021;12:688625.
4. Terlizzi M, Colarusso C, Somma P, De Rosa I, Panico L, Pinto A, Sorrentino R. S1P-induced TNF-α and IL-6 release from PBMCs exacerbates lung cancer-associated inflammation. Cells. 2022;11:16.
5. Lu Z, Fu S, Li W, Gao X, Wang J. Prognostic role of C-reactive protein to albumin ratio in lung cancer: An updated systematic review and meta-analysis. Chronic Dis Transl Med. 2024;10(1):31–9.
6. Domagala-Kulawik J. The role of the immune system in non-small cell lung carcinoma and potential for therapeutic intervention. Transl Lung Cancer Res. 2015;4(2):177–90.
7. Stankovic B, Bjørhovde HAK, Skarshaug R, Aamodt H, Frafjord A, Müller E, Hammarström C, Beraki K, Bækkevold ES, Woldbæk PR, et al. Immune cell composition in human non-small cell lung cancer. Front Immunol. 2018;9:3101.
8. Kargl J, Busch SE, Yang GH, Kim KH, Hanke ML, Metz HE, Hubbard JJ, Lee SM, Madtes DK, McIntosh MW, et al. Neutrophils dominate the immune cell composition in non-small cell lung cancer. Nat Commun. 2017;8:14381.

9. Schuurbiers OC, Meijer TW, Kaanders JH, Looijen-Salamon MG, de Geus-Oei LF, van der Drift MA, van der Heijden EH, Oyen WJ, Visser EP, Span PN, et al. Glucose metabolism in NSCLC is histology-specific and diverges the prognostic potential of 18FDG-PET for adenocarcinoma and squamous cell carcinoma. J Thorac Oncol. 2014;9(10):1485–93.
10. Lu P, Xiong L, Zhang Z, Ma Y, Liang X, Zhang X, Xu H, Yin Z, Wei S, Xiong Z, et al. Prognostic value of lipid metabolism-related genes and serum ApoA1 in patients with NSCLC. J Clin Oncol. 2022;40(16):e21040–e21040.
11. Madama D, Martins R, Pires AS, Botelho MF, Alves MG, Abrantes AM, Cordeiro CR. Metabolomic Profiling in Lung Cancer: A Systematic Review. Metabolites. 2021;11(9):97.
12. Cury SS, de Moraes D, Oliveira JS, Freire PP, Dos Reis PP, Batista ML Jr, Hasimoto ÉN, Carvalho RF. Low muscle mass in lung cancer is associated with an inflammatory and immunosuppressive tumor microenvironment. J Transl Med. 2023;21(1):116.
13. Pine SR, Mechanic LE, Enewold L, Chaturvedi AK, Katki HA, Zheng YL, Bowman ED, Engels EA, Caporaso NE, Harris CC. Increased levels of circulating interleukin 6, interleukin 8, C-reactive protein, and risk of lung cancer. J Natl Cancer Inst. 2011;103(14):1112–22.
14. Fridman WH, Pagès F, Sautès-Fridman C, Galon J. The immune contexture in human tumours: impact on clinical outcome. Nat Rev Cancer. 2012;12(4):298–306.
15. Faubert B, Li KY, Cai L, Hensley CT, Kim J, Zacharias LG, Yang C, Do QN, Doucette S, Burguete D, et al. Lactate metabolism in human lung tumors. Cell. 2017;171(2):358-371.e359.
16. May T, Clement MS, Halait H, Kohlmann A, Kohlmann M, Lai J, Lee N, Li-Sucholeiki X, Meldgaard P, Joshi S, et al. Performance characteristics of a polymerase chain reaction-based assay for the detection of EGFR mutations in plasma cell-free DNA from patients with non-small cell lung cancer using cell-free DNA collection tubes. PLoS ONE. 2024;19(4): e0295987.
17. La Salvia A, Meyer ML, Hirsch FR, Kerr KM, Landi L, Tsao MS, Cappuzzo F. Rediscovering immunohistochemistry in lung cancer. Crit Rev Oncol Hematol. 2024;89:104401.
18. Liu H, He S, Tan L, Li M, Chen C, Tan R. Disulfidptosis-related long non-coding RNAs predict prognosis and indicate therapeutic response in non-small cell lung carcinoma. Oncologie. 2024;26(1):151–65.
19. Li H, Lei Y, Li G, Huang Y. Identification of tumor-suppressor genes in lung squamous cell carcinoma through integrated bioinformatics analyses. Oncol Res. 2023;32(1):187.
20. Liang H, Li Y, Qu Y, Zhang L. Leveraging diverse cell-death patterns to predict the clinical outcome of immune checkpoint therapy in lung adenocarcinoma: Based on muti-omics analysis and vitro assay. Oncol Res. 2023;32(2):393.
21. Zhao JH, Stacey D, Eriksson N, Macdonald-Dunlop E, Hedman ÅK, Kalnapenkis A, Enroth S, Cozzetto D, Digby-Bell J, Marten J, et al. Genetics of circulating inflammatory proteins identifies drivers of immune-mediated disease risk and therapeutic targets. Nat Immunol. 2023;24(9):1540–51.
22. Orrù V, Steri M, Sidore C, Marongiu M, Serra V, Olla S, Sole G, Lai S, Dei M, Mulas A, et al. Complex genetic signatures in immune cells underlie autoimmunity and inform therapy. Nat Genet. 2020;52(10):1036–45.
23. Chen Y, Lu T, Pettersson-Kymmer U, Stewart ID, Butler-Laporte G, Nakanishi T, Cerani A, Liang KYH, Yoshiji S, Willett JDS, et al. Genomic atlas of the plasma metabolome prioritizes metabolites implicated in human diseases. Nat Genet. 2023;55(1):44–53.
24. Verbanck M, Chen CY, Neale B, Do R. Detection of widespread horizontal pleiotropy in causal relationships inferred from Mendelian randomization between complex traits and diseases. Nat Genet. 2018;50(5):693–8.
25. Vlaic BA, Vlaic A, Russo IR, Colli L, Bruford MW, Odagiu A, Orozco-terWengel P, Climgen C. Analysis of genetic diversity in Romanian carpatina goats using SNP genotyping data. Animals (Basel). 2024;14(4):9.
26. Papadimitriou N, Dimou N, Tsilidis KK, Banbury B, Martin RM, Lewis SJ, Kazmi N, Robinson TM, Albanes D, Aleksandrova K, et al. Physical activity and risks of breast and colorectal cancer: a Mendelian randomisation analysis. Nat Commun. 2020;11(1):597.
27. Burgess S, Butterworth A, Thompson SG. Mendelian randomization analysis with multiple genetic variants using summarized data. Genet Epidemiol. 2013;37(7):658–65.
28. Bowden J, Davey Smith G, Burgess S. Mendelian randomization with invalid instruments: effect estimation and bias detection through Egger regression. Int J Epidemiol. 2015;44(2):512–25.
29. Bowden J, Davey Smith G, Haycock PC, Burgess S. Consistent estimation in mendelian randomization with some invalid instruments using a weighted median estimator. Genet Epidemiol. 2016;40(4):304–14.
30. Burgess S, Thompson SG. Avoiding bias from weak instruments in Mendelian randomization studies. Int J Epidemiol. 2011;40(3):755–64.
31. Burgess S, Scott RA, Timpson NJ, Davey Smith G, Thompson SG. Using published data in Mendelian randomization: a blueprint for efficient identification of causal risk factors. Eur J Epidemiol. 2015;30(7):543–52.
32. Burgess S, Bowden J, Fall T, Ingelsson E, Thompson SG. Sensitivity analyses for robust causal inference from Mendelian randomization analyses with multiple genetic variants. Epidemiology. 2017;28(1):30–42.
33. Mangiola S, Doyle MA, Papenfuss AT. Interfacing Seurat with the R tidy universe. Bioinformatics. 2021;37(22):4100–7.
34. Aran D, Looney AP, Liu L, Wu E, Fong V, Hsu A, Chak S, Naikawadi RP, Wolters PJ, Abate AR, et al. Reference-based analysis of lung single-cell sequencing reveals a transitional profibrotic macrophage. Nat Immunol. 2019;20(2):163–72.
35. Jin S, Guerrero-Juarez CF, Zhang L, Chang I, Ramos R, Kuan CH, Myung P, Plikus MV, Nie Q. Inference and analysis of cell-cell communication using Cell Chat. Nat Commun. 2021;12(1):1088.
36. Szklarczyk D, Gable AL, Lyon D, Junge A, Wyder S, Huerta-Cepas J, Simonovic M, Doncheva NT, Morris JH, Bork P, et al. STRING v11: protein-protein association networks with increased coverage, supporting functional discovery in genome-wide experimental datasets. Nucleic Acids Res. 2019;47(D1):D607-d613.
37. Ewald JD, Zhou G, Lu Y, Kolic J, Ellis C, Johnson JD, Macdonald PE, Xia J. Web-based multi-omics integration using the Analyst software suite. Nat Protoc. 2024;45:67.
38. Kastenhuber ER, Lowe SW. Putting p53 in context. Cell. 2017;170(6):1062–78.
39. Jamal-Hanjani M, Wilson GA, McGranahan N, Birkbak NJ, Watkins TBK, Veeriah S, Shafi S, Johnson DH, Mitter R, Rosenthal R, et al. Tracking the evolution of non-small-cell lung cancer. N Engl J Med. 2017;376(22):2109–21.
40. Chen S, Wang X, Yang N, Song Y, Cheng H, Sun Y. p53 exerts anticancer effects by regulating enhancer formation and activity. J Biomed Res. 2024;56:1–14.

41. Deben C, Wouters A, de Beeck K, van Bossche J, Jacobs J, Zwaenepoel K, Peeters M, Van Meerbeeck J, Lardon F, Rolfo C, et al. The MDM2-inhibitor Nutlin-3 synergizes with cisplatin to induce p53 dependent tumor cell apoptosis in non-small cell lung cancer. Oncotarget. 2015;6(26):22666–79.
42. Khodarev NN, Roizman B, Weichselbaum RR. Molecular pathways: interferon/stat1 pathway: role in the tumor resistance to genotoxic stress and aggressive growth. Clin Cancer Res. 2012;18(11):3015–21.
43. Yu SK, Yu T, Wang YM, Sun A, Liu J, Lu KH. CCT6A facilitates lung adenocarcinoma progression and glycolysis via STAT1/HK2 axis. J Transl Med. 2024;22(1):460.
44. Yuan X, Wu H, Han N, Xu H, Chu Q, Yu S, Chen Y, Wu K. Notch signaling and EMT in non-small cell lung cancer: biological significance and therapeutic application. J Hematol Oncol. 2014;7:87.
45. Sun J, Dong M, Xiang X, Zhang S, Wen D. Notch signaling and targeted therapy in non-small cell lung cancer. Cancer Lett. 2024;585: 216647.
46. Leonetti A, Facchinetti F, Minari R, Cortellini A, Rolfo CD, Giovannetti E, Tiseo M. Notch pathway in small-cell lung cancer: from preclinical evidence to therapeutic challenges. Cell Oncol (Dordr). 2019;42(3):261–73.
47. Ying S, Meng Q, Zeibecoglou K, Robinson DS, Macfarlane A, Humbert M, Kay AB. Eosinophil chemotactic chemokines (eotaxin, eotaxin-2, RANTES, monocyte chemoattractant protein-3 (MCP-3), and MCP-4), and C-C chemokine receptor 3 expression in bronchial biopsies from atopic and nonatopic (Intrinsic) asthmatics. J Immunol. 1999;163(11):6321–9.
48. Ghaffari S, Rezaei N. Eosinophils in the tumor microenvironment: implications for cancer immunotherapy. J Transl Med. 2023;21(1):551.
49. Halwani R, Al-Muhsen S, Al-Jahdali H, Hamid Q. Role of transforming growth factor-β in airway remodeling in asthma. Am J Respir Cell Mol Biol. 2011;44(2):127–33.
50. Lv J, Xiong Y, Li W, Cui X, Cheng X, Leng Q, He R. IL-37 inhibits IL-4/IL-13-induced CCL11 production and lung eosinophilia in murine allergic asthma. Allergy. 2018;73(8):1642–52.
51. Odaka M, Matsukura S, Kuga H, Kokubu F, Kasama T, Kurokawa M, Kawaguchi M, Ieki K, Suzuki S, Watanabe S, et al. Differential regulation of chemokine expression by Th1 and Th2 cytokines and mechanisms of eotaxin/CCL-11 expression in human airway smooth muscle cells. Int Arch Allergy Immunol. 2007;143(1):84–8.
52. Singh SR, Sutcliffe A, Kaur D, Gupta S, Desai D, Saunders R, Brightling CE. CCL2 release by airway smooth muscle is increased in asthma and promotes fibrocyte migration. Allergy. 2014;69(9):1189–97.
53. Kodali RB, Kim WJ, Galaria II, Miller C, Schecter AD, Lira SA, Taubman MB. CCL11 (Eotaxin) induces CCR3-dependent smooth muscle cell migration. Arterioscler Thromb Vasc Biol. 2004;24(7):1211–6.
54. Nguyen T, Kirsch BJ, Asaka R, Nabi K, Quinones A, Tan J, Antonio MJ, Camelo F, Li T, Nguyen S, et al. Uncovering the role of N-acetyl-aspartyl-glutamate as a glutamate reservoir in cancer. Cell Rep. 2019;27(2):491-501.e496.
55. Zhang C, Quinones A, Le A. Metabolic reservoir cycles in cancer. Semin Cancer Biol. 2022;86(Pt 3):180–8.
56. Evans JC, Malhotra M, Cryan JF, O'Driscoll CM. The therapeutic and diagnostic potential of the prostate specific membrane antigen/glutamate carboxypeptidase II (PSMA/GCPII) in cancer and neurological disease. Br J Pharmacol. 2016;173(21):3041–79.
57. Zhou J, Neale JH, Pomper MG, Kozikowski AP. NAAG peptidase inhibitors and their potential for diagnosis and therapy. Nat Rev Drug Discov. 2005;4(12):1015–26.
58. Long PM, Moffett JR, Namboodiri AMA, Viapiano MS, Lawler SE, Jaworski DM. N-acetylaspartate (NAA) and N-acetylaspartylglutamate (NAAG) promote growth and inhibit differentiation of glioma stem-like cells. J Biol Chem. 2013;288(36):26188–200.
59. Asaka R, Le A. Dual role of N-acetyl-aspartyl-glutamate metabolism in cancer monitor and therapy. Mol Cell Oncol. 2019;6(5): e1627273.
60. de Blay F, Gherasim A, Domis N, Choual I, Bourcier T. Efficacy of N-acetyl aspartyl glutamic acid versus fluorometholone for treating allergic conjunctivitis in an environmental exposure chamber. Clin Exp Allergy. 2022;52(9):1091–100.
61. Lapalus P, Moulin G, Bayer V, Fredj-Reygrobellet D, Elena PP. Effects of a new anti-allergic agent: the magnesium salt of N-acetyl-aspartyl-glutamic acid on experimental allergic inflammation of the rabbit eye. Curr Eye Res. 1986;5(7):517–22.
62. Zhang S, Sun Y. Targeting CDC34 E2 ubiquitin conjugating enzyme for lung cancer therapy. EBioMedicine. 2020;54: 102718.
63. Zhang Z, Liu P, Wang J, Gong T, Zhang F, Ma J, Han N. Ubiquitin-conjugating enzyme E2C regulates apoptosis-dependent tumor progression of non-small cell lung cancer via ERK pathway. Med Oncol. 2015;32(5):149.
64. Tang XK, Wang KJ, Tang YK, Chen L. Effects of ubiquitin-conjugating enzyme 2C on invasion, proliferation and cell cycling of lung cancer cells. Asian Pac J Cancer Prev. 2014;15(7):3005–9.
65. Ju Y, Xu T, Zhang H, Yu A. FOXO1-dependent DNA damage repair is regulated by JNK in lung cancer cells. Int J Oncol. 2014;44(4):1284–92.
66. Liu Z, Huang M, Hong Y, Wang S, Xu Y, Zhong C, Zhang J, Zhuang Z, Shan S, Ren T. Isovalerylspiramycin I suppresses non-small cell lung carcinoma growth through ROS-mediated inhibition of PI3K/AKT signaling pathway. Int J Biol Sci. 2022;18(9):3714–30.
67. Sun T, Zhang J, Deng B, Fan X, Long T, Jin H, Tao S, Kang P, Tan Q. FOXO1 and FOXO3a sensitize non-small-cell lung cancer cells to cisplatin-induced apoptosis independent of Bim. Acta Biochim Biophys Sin (Shanghai). 2020;52(12):1348–59.
68. Ebrahimnezhad M, Natami M, Bakhtiari GH, Tabnak P, Ebrahimnezhad N, Yousefi B, Majidinia M. FOXO1, a tiny protein with intricate interactions: Promising therapeutic candidate in lung cancer. Biomed Pharmacother. 2023;169: 115900.
69. Huang WY, Lin YS, Lin YC, Nieh S, Chang YM, Lee TY, Chen SF, Yang KD. Cancer-Associated Fibroblasts Promote Tumor Aggressiveness in Head and Neck Cancer through Chemokine Ligand 11 and C-C Motif Chemokine Receptor 3 Signaling Circuit. Cancers (Basel). 2022;14(13):897.
70. Jin L, Liu WR, Tian MX, Jiang XF, Wang H, Zhou PY, Ding ZB, Peng YF, Dai Z, Qiu SJ, et al. CCL24 contributes to HCC malignancy via RhoB-VEGFA-VEGFR2 angiogenesis pathway and indicates poor prognosis. Oncotarget. 2017;8(3):5135–48.
71. Lin S, Zhang X, Huang G, Cheng L, Lv J, Zheng D, Lin S, Wang S, Wu Q, Long Y, et al. Myeloid-derived suppressor cells promote lung cancer metastasis by CCL11 to activate ERK and AKT signaling and induce epithelial-mesenchymal transition in tumor cells. Oncogene. 2021;40(8):1476–89.
72. Bekaert S, Rocks N, Vanwinge C, Noel A, Cataldo D. Asthma-related inflammation promotes lung metastasis of breast cancer cells through CCL11-CCR3 pathway. Respir Res. 2021;22(1):61.
73. Zanini D, Manfredi LH, Pelinson LP, Pimentel VC, Cardoso AM, Carmo Araújo Gonçalves VD, Santos CBD, Gutierres JM, Morsch VM, Leal DBR, et al. ADA activity is decreased in lymphocytes from patients with advanced stage of lung cancer. Med Oncol. 2019;36(9):78.

74. Marković I, Savvides SN. Modulation of signaling mediated by TSLP and IL-7 in inflammation, autoimmune diseases, and cancer. Front Immunol. 2020;11:1557.
75. Qu H, Liu X, Jiang T, Huang G, Cai H, Xing D, Mao Y, Zheng X. Integration analysis using bioinformatics and experimental validation on the clinical and biological significance of TSLP in cancers. Cell Signal. 2023;111: 110874.
76. Wakabayashi O, Yamazaki K, Oizumi S, Hommura F, Kinoshita I, Ogura S, Dosaka-Akita H, Nishimura M. CD4+ T cells in cancer stroma, not CD8+ T cells in cancer cell nests, are associated with favorable prognosis in human non-small cell lung cancers. Cancer Sci. 2003;94(11):1003–9.
77. Kwiecień I, Rutkowska E, Sokołowski R, Bednarek J, Raniszewska A, Jahnz-Różyk K, Rzepecki P, Domagała-Kulawik J. Effector Memory T Cells and CD45RO+ regulatory T cells in metastatic vs non-metastatic lymph nodes in lung cancer patients. Front Immunol. 2022;13:864497.
78. Bremnes RM, Al-Shibli K, Donnem T, Sirera R, Al-Saad S, Andersen S, Stenvold H, Camps C, Busund LT. The role of tumor-infiltrating immune cells and chronic inflammation at the tumor site on cancer development, progression, and prognosis: emphasis on non-small cell lung cancer. J Thorac Oncol. 2011;6(4):824–33.
79. Chen J, Tan Y, Sun F, Hou L, Zhang C, Ge T, Yu H, Wu C, Zhu Y, Duan L, et al. Single-cell transcriptome and antigen-immunoglobin analysis reveals the diversity of B cells in non-small cell lung cancer. Genome Biol. 2020;21(1):152.
80. Al-Shibli KI, Donnem T, Al-Saad S, Persson M, Bremnes RM, Busund LT. Prognostic effect of epithelial and stromal lymphocyte infiltration in non-small cell lung cancer. Clin Cancer Res. 2008;14(16):5220–7.
81. Pelletier MP, Edwardes MD, Michel RP, Halwani F, Morin JE. Prognostic markers in resectable non-small cell lung cancer: a multivariate analysis. Can J Surg. 2001;44(3):180–8.